OXFORD Toxicology Research

*Toxicology Research*, 2020, **9**, 454–460

**doi: 10.1093/toxres/tfaa036**
Advance Access Publication Date: 3 July 2020
Paper

PAPER

# Silica nanoparticles induce unfolded protein reaction mediated apoptosis in spermatocyte cells

Lihua Ren,[1,2] Jianhui Liu,[2,3] Jialiu Wei,[4] Yefan Du,[1] Kaiyue Zou,[1] Yongyang Yan,[1] Zhihao Wang,[1] Linruo Zhang,[1] Tong Zhang,[1] Hong Lu,[1] Xianqing Zhou[2,3,*] and Zhiwei Sun[2,3]

[1]Division of Maternal and Child Nursing, School of Nursing, Peking University Health Science Centre, No 38 Xueyuan Road, Haidian District, Beijing 100191, China, [2]Department of Toxicology and Hygienic Chemistry, School of Public Health, Capital Medical University, No 10 Xi Tou Tiao, Fengtai District, Beijing 100069, China, [3]Beijing Key Laboratory of Environmental Toxicology, Capital Medical University, No 10 Xi Tou Tiao, Fengtai District, Beijing 100069, China and [4]Department of Epidemiology, State Key Laboratory of Cardiovascular Disease, Fuwai Hospital, National Center for Cardiovascular Diseases, Chinese Academy of Medical Sciences and Peking Union Medical College, No 167 North Lishi Road, Xicheng District, Beijing 100037, China

*Correspondence address. Department of Toxicology and Hygienic Chemistry, School of Public Health, Capital Medical University, Beijing 100069, China. Tel: 8610-83916539; Fax: 8610-59784719; E-mail: xqzhou2@163.com; xqzhou@ccmu.edu.cn



## Abstract

With increasing air pollution, silica nanoparticles (SiNPs), as a main inorganic member of $PM_{2.5}$, have gained increasing attention to its reproductive toxicity. Most existing studies focused on the acute exposure, while data regarding the chronic effect of SiNPs on reproduction is limited. Therefore, this study was designed to evaluate the chronic toxicity of SiNPs on spermatocyte cells. The cells were continuously exposed to SiNPs for 1, 10, 20 and 30 generations at dose of 5 μg/ml SiNPs for 24 h per generation after attachment. The results showed that with the increasing generations of the exposure, SiNPs decreased the viability of spermatocyte cells, induced apoptosis and increased the level of reactive oxygen species in spermatocyte cells. Moreover, SiNPs increased the protein expression of GRP-78, p-PERK, IRE1$\alpha$, ATF6 and Cleaved caspase-3 in spermatocyte cells, suggesting that SiNPs improved unfolded protein response (UPR) and apoptosis. The present results indicated that the long-term and low-dose exposure to SiNPs could induce apoptosis by triggering ROS-mediated UPR in spermatocyte cells.

**Key words:** silica nanoparticles (SiNPs), spermatocyte cells, apoptosis, unfolded protein response

## Introduction

In recent decades, the incidence of infertility has raised sharply [1]. It has been reported that about 40% of infertility was caused by male factor [2]. In addition, numerous studies have proved that environmental pollution is associated with increased infertility and spermatogenesis disorder [3–5]. As air pollution increases, silica nanoparticles (SiNPs), the main inorganic components of $PM_{2.5}$ [6, 7], are present in large quantities in the environment. Therefore, with the aggravation of environmental pollution, the effect of SiNPs on male reproductive function deserves to be stressed.

After respiratory exposure, SiNPs can migrate from lung to the extrapulmonary organs [8, 9]. SiNPs were also appeared in the cytoplasm and nucleus of spermatocyte cells after

**Received:** 26 January 2020; **Revised:** 14 May 2020; **Accepted:** 15 May 2020

intravenously injected [10]. Therefore, SiNPs might induce the damage of male reproductive system. A study in 2014 illustrated that exposure to nanoparticles resulted in decreased sperm motility, decreased number of Leydig cells and altered sperm morphology in rats [11]. Subsequently, researchers found that exposure to SiNPs could impair spermatogenesis, decrease sperm motility and sperm concentration and increase sperm malformation in rainbow trout and mice [12, 13]. Our previous studies have also shown that SiNPs damage spermatogenic cells and lower the quality and quantity of sperm in rats [14, 15]. Therefore, more attention should be paid to the mechanism of SiNPs-induced lesion in spermatogenic cells.

The unfolded protein response (UPR) may play a very important role in SiNPs' reproductive toxicity. UPR happens in a kind of endoplasmic reticulum (ER) [16]. The over accumulation of unfolded or misfolded proteins in the ER can cause ER stress and trigger UPR [16]. Researchers found that SiNPs could increase the protein expression of BiP in Huh7 cells [17] and induce UPR through the activation of the EIF2AK3 and ATF6 UPR pathways in hepatocytes [18]. Moreover, SiNPs could induce apoptosis through reactive oxygen species (ROS)-mediated ER stress [19]. In our previous studies, it is proved that SiNPs could induce apoptosis in spermatogenic cells by activating the death receptor pathway resulting from oxidative stress in male mice [14]. Furthermore, SiNPs induce apoptosis through microRNA-2861 targeting fas/fasl/ripk1 in the death receptor pathway via oxidative stress of spermatocyte cells [20]. Above all, SiNPs can induce apoptosis in spermatogenic cells via oxidative stress. UPR can be triggered by oxidative stress [19]. However, the role of UPR in SiNPs-induced apoptosis in spermatogenic cells remains unclear.

In previous studies, the damage of male reproductive function was focused on acute exposure to SiNPs [12, 21], while studies on the chronic effects of SiNPs are limited. Therefore, to get a further insight into the effect of long-term exposure to low-dose SiNPs on reproduction, this study was designed to evaluate the toxicity of exposure to SiNPs for 30 generations in spermatocyte cells and the role of UPR in SiNPs-induced apoptosis.

## Materials and Methods

### Experimental design

Spermatocyte cells (GC-2spd) were obtained from Guangzhou Jennio Biotech Co., Ltd. The cells were cultured in 10 ml mixture consisting of 9 ml DMEM (Genview, USA) medium, 1 ml fetal bovine serum (Gibco, USA) with 1000 U penicillin and 1000 μg streptomycin in a 5% $CO_2$ humidified environment at 37°C. Spermatocyte cells were seeded in 100 mm diameter cell culture plates at each passage. Three similar plates were used in each group. For tests, the cells were seeded in six-well plates [except Cell Counting Kit-8 (CCK8) assay using 96-well plates] at a density of $1 \times 10^5$ cells/ml. Six replicate wells were used in each detection. The cells were divided into two groups (control group and 5 μg/ml SiNPs group) in the stable growth phase. The cells in control group were cultured in an equivalent volume of DMEM without SiNPs. The cells in 5 μg/ml SiNPs group were exposed to SiNPs for 24 h after attachment in each generation, and were, respectively, passed for 1, 10, 20 and 30 times in total. In addition, after exposure to SiNPs for 30 generations, the cells in 5 μg/ml SiNPs group were treated with 10 mM of 4-phenyl butyric acid (4PBA, an inhibitor of ER stress and UPR) for 6 h to detect the role of ER stress in reproductive toxicity induced by SiNPs.

### SiNP preparation and characterization

SiNPs were prepared according to the Stöber method. Firstly, the researchers mixed ethanol solution (50 ml), ammonia (2 ml) and water (1 ml). Secondly, with continuous stirring (150 r/min), tetraethyl orthosilicate (2.5 ml) was added and the mixed liquor was kept at 40°C for 12 h. Thirdly, the particles were isolated by centrifugation (Eppendorf, 5810R, Germany) with the centrifuge rotor radius (173 mm) (12 000 r/min, 15 min), washed three times with deionized water and then dispersed in 50 ml of deionized water. With the help of transmission electron microscope (TEM) (JEOL JEM2100, Japan), the shape and distribution of SiNPs were observed. The size of 500 particles was counted by ImageJ software.

### The detection of cell viability

The cell viability was measured in the 1st, 10th, 20th and 30th generations by CCK8 (Dingguo Changsheng bioengineering Institute, China). After exposed to SiNPs, spermatocyte cells were seeded into the 96-well plate at a concentration of $1 \times 10^5$ cells/ml. The cell viability was then detected at 450 nm by a microplate reader (Themo Multiscan MK3, USA), and the absorbance was detected.

### The detection of ROS

The species of reactive oxygen were measured in the 1st, 10th, 20th and 30th generations. After exposure to SiNPs, spermatocyte cells were seeded into the 96-well plate at a concentration of $1 \times 10^5$ cells/ml. The cells were washed by phosphate buffer saline (PBS) and incubated away from light at 37°C with DCFH-DA working solution for 30 min. Then, the cells were washed twice with cold PBS. At last, the absorbance was measured by microplate reader (Themo Multiscan MK3, USA) using the excitation wavelength of 485 nm and the emission wavelength of 525 nm.

### Ultrastructure of spermatocyte cells

After exposure to SiNPs for 30 generations, the ultrastructure of spermatocyte cells was observed. The cells were washed by PBS, collected and centrifuged, and the cell pellets were fixed in 2.5% glutaraldehyde for 3 h. Subsequently, the fixed pellets were washed with 0.1 M phosphate buffer, embedded in a 2% agarose gel, post-fixed in a 4% osmium tetroxide solution, stained with 0.5% uranyl acetate and dehydrated in a graded series of ethanol. The cell pellets were then embedded in an epoxy resin, and the resin was polymerized at 60°C for 48 h. The stained ultrathin sections were imaged by a TEM (JEOL JEM2100, Japan).

### The detection of the protein expression

Firstly, the total protein was isolated from spermatocyte cells by the Total Protein Rapid Extraction Kit (Jiancheng Bioengineering Institute) and quantified by the protein quantification kit (KeyGen Biotechnology). SDS-polyacrylamide gels (12%) were used to isolate 25 μg of the lysate proteins. And then, the proteins were transport to the nitrocellulose (NC) membranes (Gelman Laboratory, USA). After sealing with TBST and BSA for 1.5 h, the NC membranes were incubated with p-PERK, GRP-78, IRE1$\alpha$, ATF6 (1:500, rabbit antibodies, Boster Biological Technology Co., Ltd, China) and Caspase 3 (1:1000, rabbit antibodies, Cell Signaling

Technology, Beverly, MA, USA) at room temperature for 1 h and overnight at 4°C. The membranes were washed and incubated with the secondary antibody for 1 h (1:15000, anti-rabbit IgG, ZSGB-BIO, Beijing, China). Ultimately, using the chemiluminescence imaging system (Tanon 5200; Tanon, Guangzhou, People's Republic of China), the antibody-bound proteins were detected by the enhanced chemiluminescence reagent (Thermo Fisher Scientifc, Waltham, MA, USA).

### The detection of cell apoptosis

Cells apoptosis was detected by the Annexin V-propidium iodide (PI) apoptosis detection kit (KeyGen, China). After exposure to 5 μg/ml SiNPs for 30 generations, the cells were washed, trypsinized, collected and centrifuged. Then, the cells were resuspended with a binding buffer, 5 μl Annexin V-FITC and 5 μl PI. The apoptotic cells were detected by flow cytometry (Becton Dickinson, USA). Afterwards, based on the properties of forward and side scattering, the cell population was calculated. The cells in the quadrant of FITC negative and PI negative were considered to be living cells, those in the quadrant of FITC positive and PI negative were early apoptotic cells, those in the quadrant of FITC positive and PI positive were late apoptotic cells and those in the quadrant of FITC negative and PI positive were cells fragment.

### Statistical analysis

All the statistical analyses were performed by using the statistical software SPSS20.0. One-way analysis of variance was used to analyze differences in multiple groups, followed by the least significant difference test in two groups for apoptosis. The independent sample *t*-test was used to test mean differences between the control group and the SiNPs group at the same generations for viability, oxidative stress and UPR. All values were expressed as mean ± standard deviation and difference was signally at $P < 0.05$.

## Results

### The characterization of SiNPs

The TEM observation revealed that the shape of SiNPs is similar to spherical shape, and the size distribution is uniform (Fig. 1). The average diameter measured by Image J software is 57.66 ± 7.30 nm. SiNPs are of not only good monodispersity but also stability in DMEM and distilled water over time. The information of hydrodynamic sizes and zeta potential can be obtained from our previous study [20].

### The changes of viability and oxidative stress in spermatocyte cells

Cell viability was measured after exposure to SiNPs for 1, 10, 20 and 30 generations. The results showed that the viability in the control group and the SiNPs group decreased with the increase of exposure time. However, the decline in the SiNPs group was more severe. At the 20th and 30th generations, the cell viability in the SiNPs group was significantly lower than that in the control group (Fig. 2A).

After exposure to SiNPs for 1, 10, 20 and 30 generations, the activity of ROS was detected. With the exposure time increase, the level of ROS was elevated. Furthermore, at the 20th and 30th generation, the ROS level in the SiNPs group was significantly higher than that in the control group (Fig. 2B).

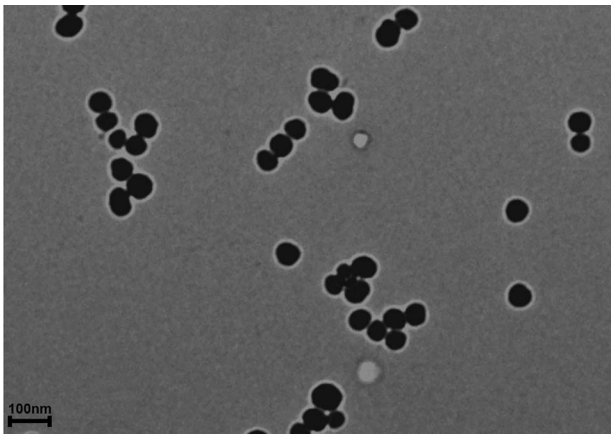


**Figure 1**: The characterization of SiNPs. Notes: The TEM images of SiNPs.

### The changes of ultrastructure in spermatocyte cells

The ultrastructure of GC-2spd was observed by TEM after exposure to SiNPs for 30 generations. The rough ER was regularly shaped and the mitochondrial cristae were clear in the control group (Fig. 3A and B). In the SiNPs group, the rough ER swelled, and the mitochondrial crista disappeared (Fig. 3C and D). Moreover, the SiNPs were found in the cells of the SiNPs group (Fig. 3E and F).

### The changes of unfolded protein reaction in spermatocyte cells

In order to obtain the status of UPR in spermatocyte cells, the proteins expression of GRP-78, p-PERK, IRE1$\alpha$ and ATF6 of GC-2spd cells were detected in the 1st, 10th, 20th and 30th generation. With the increase of generation, the proteins expression of GRP-78, p-PERK, IRE1$\alpha$ and ATF6 gradually increased. In the 20th generation, only the expression of p-PERK was significantly higher in the 5 μg/ml SiNPs group than that in the control group. In the 30th generation, the protein expressions of GRP-78, p-PERK, IRE1$\alpha$ and ATF6 were significantly higher in the 5 μg/ml SiNPs group than those in the control group (Fig. 4).

### The changes of spermatocyte cells apoptosis

The apoptosis of spermatocyte cells was detected by flow cytometry and western blot. After exposure to SiNPs for 30 generations, the level of apoptosis of GC-2spd cells and the expression of Cleaved caspase-3 in the 5 μg/ml SiNPs group were significantly higher than those in the control group. Compared with the 5 μg/ml SiNPs group, the apoptosis level of GC-2spd cells and the expression of Cleaved caspase-3 in the 5 μg/ml SiNPs group with 4PBA were significantly decreased compared with 5 μg/ml SiNPs group (Fig. 5), which indicated that 4PBA, a UPR inhibitor, antagonized SiNPs-induced apoptosis and increased expression of Cleaved caspase-3 in spermatocyte cells.

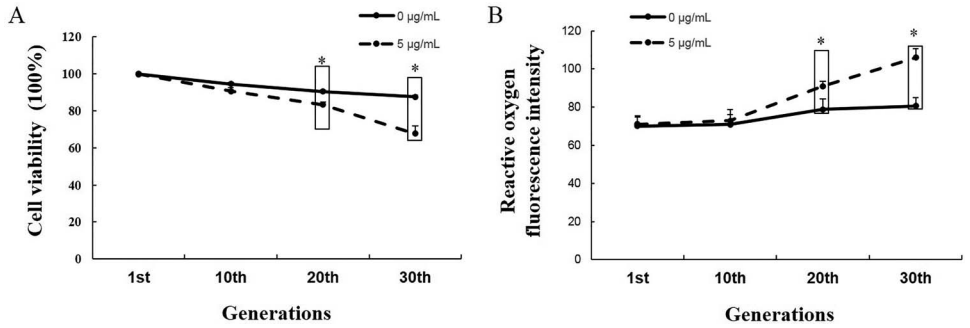


**Figure 2**: The effects on the viability and oxidative stress in spermatocyte cells after exposure to SiNPs for 1, 10, 20 and 30 generations. Notes: **A**: Cell viability. **B**: Reactive oxygen fluorescence intensity. SiNPs inhibited the cell viability and hasten the development of ROS. $^{*}P < 0.05$ represents significantly difference between the control group and the 5 μg/ml SiNPs group in the same generation.

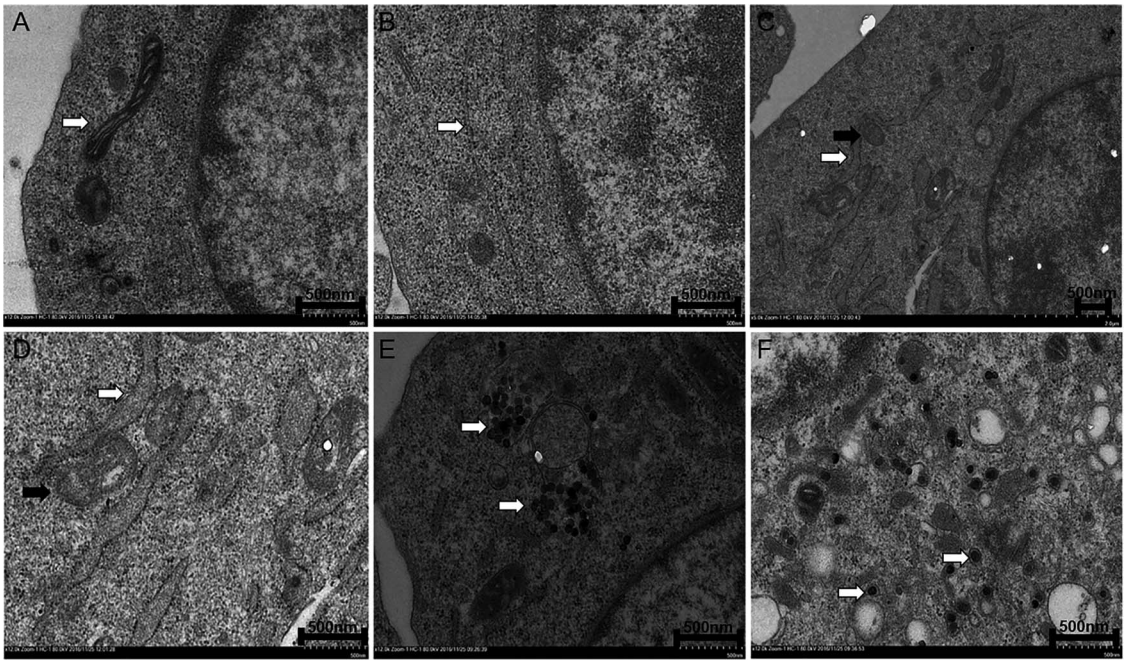


**Figure 3**: The changes of ultrastructure in spermatocyte cells after exposure to SiNPs for 30 generations. Notes: The figure shows the TEM images of spermatocyte cells. SiNPs disturbed the ultrastructure of mitochondrion and ER. **A**, **B**: The control group. **C**, **D**, **E**, **F**: The 5 μg/ml SiNPs group. A: The white arrow represents mitochondrion. B: The white arrow represents ER. C, D: The white arrow represents ER. B: The black arrow represents mitochondrion. E, F: The white arrow represents silica nanoparticles.

## Discussion

With the aggravation of environmental pollution, the incidence of infertility continues to increase, and the quantity and quality of human sperm declines in worldwide [22, 23]. As one of the components of environmental pollution, SiNPs exist in low doses in the environment and are in long-term contact with humans. Therefore, the chronic toxicity of SiNPs effects on spermatocyte cells deserves more attention.

This study explored the long-term effects of low-dose SiNPs on spermatocyte cells. After exposure to SiNPs for 20 and 30 generations, mitochondrial swelling was observed in the spermatocyte cells. The cell viability of the spermatocyte cells gradually decreased, and the level of oxidative stress increased. These results indicated that long-term exposure to low doses of SiNPs could induce cytotoxicity in spermatocyte cells, similar to our previous findings. The previous studies have shown that after exposure for 30 generations, SiNPs can induce apoptosis and autophagy in spermatocyte cells [20, 24]. There is little useful information about the long-term effects of low-dose SiNPs on spermatocyte cells, and further study is urgently needed.

UPR may play an important role in the long-term effects of low-dose SiNPs on spermatocyte cells. UPR can regulate protein quality and enhance the ability of protein folding to maintain homeostasis [25]. GRP78 contacts unfolded and misfolded proteins to facilitate appropriate protein processing. GRP78's dissociation from PERK, IRE1$\alpha$ and ATF6 can be induced by the increase of misfolded proteins [26, 27], leading to the activation of UPR by oligomerization, autophosphorylation and/or translocation [28, 29]. In the results, with the increase of exposure time, P-PERK significantly increased in the 20th and 30th generation, and GRP78, ATF6 and IRE1$\alpha$ significantly increased in 30th generation. The results illustrated that SiNPs increased UPR in spermatocyte cells. Other researchers have proved that SiNPs can induce ROS [30, 31]. Oxidative stress can induce unfolded protein reactions. Antioxidants could alleviate unfolded protein reactions [32]. In addition, with the increase of GRP78 and PERK, UPR was activated

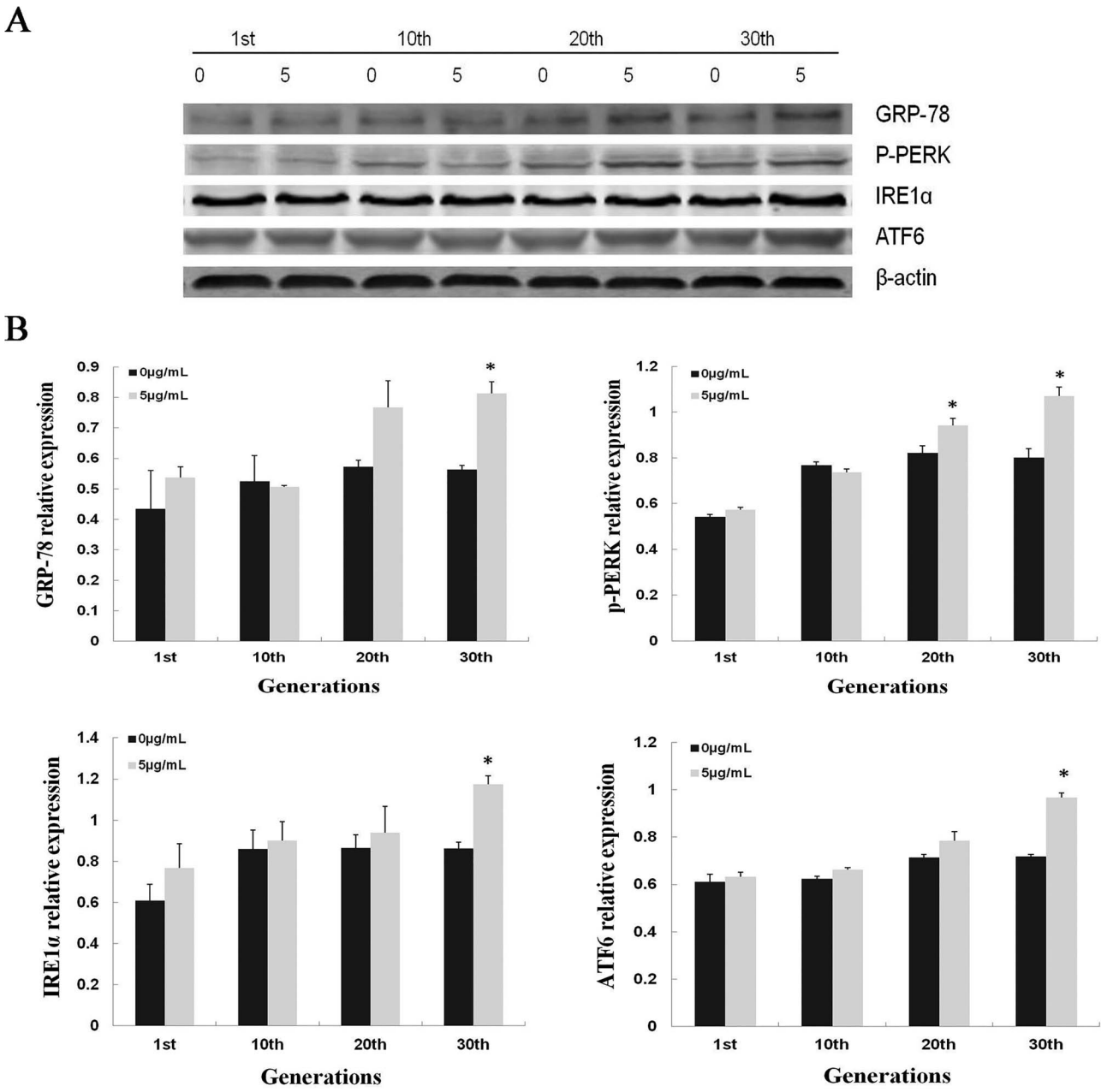


**Figure 4**: The changes of unfolded protein reaction in spermatocyte cells after exposure to SiNPs for 1, 10, 20 and 30 generations. Notes: **A**: Protein bands of GRP-78/p-PERK/IRE1$\alpha$/ATF6. **B**: The proteins expression of GRP-78/p-PERK/IRE1$\alpha$/ATF6. SiNPs hasten the development of UPR-related proteins GRP-78/p-PERK/IRE1$\alpha$/ATF6. $^{*}P < 0.05$ represents significantly difference between the control group and the 5 μg/ml SiNPs group in the same generation.

by ROS after Cd exposure in placenta [33]. As UPR increases, chloroacetic acid could trigger apoptosis in neuronal cells [34]. Consequently, SiNPs may trigger UPR via ROS in spermatocyte cells.

Long-term and low-dose SiNPs might induce spermatocyte apoptosis by UPR. In this research, the level of apoptotic spermatocyte cells increased with the increase of exposure generations. To examine the role of UPR in apoptosis, 4PBA was used to inhibit UPR. 4PBA is a small molecular compound that can facilitate protein transport in the direction of praise in the ER, reducing the load on the ER [35–37].

It is feasible that the cells were incubated with 4PBA for 1-6 h to reduce UPR in previous researches [38–41]. Therefore, we decide to conservatively use the inhibitor 4PBA for the treatment of the cells incubated with SiNPs only at the 30th generation, and the level of UPR reduced after cells incubated with 4PBA in this study, which showed the effect of inhibitor 4PBA. When using 4PBA, both spermatocyte apoptosis and the protein expression of Cleaved caspase-3 decreased. Shigemi *et al.* found in their research that methylseleninic acid could induce the apoptosis by up-regulating UPR in PEL cells [42]. UPR can induce apoptosis of $\beta$-cell in L3 rats [43]. Hence, SiNPs induced spermatocyte apoptosis by UPR. In conclusion, the results suggested that low-dose SiNPs could induce spermatocyte apoptosis by increasing UPR via activated ROS in the long term.

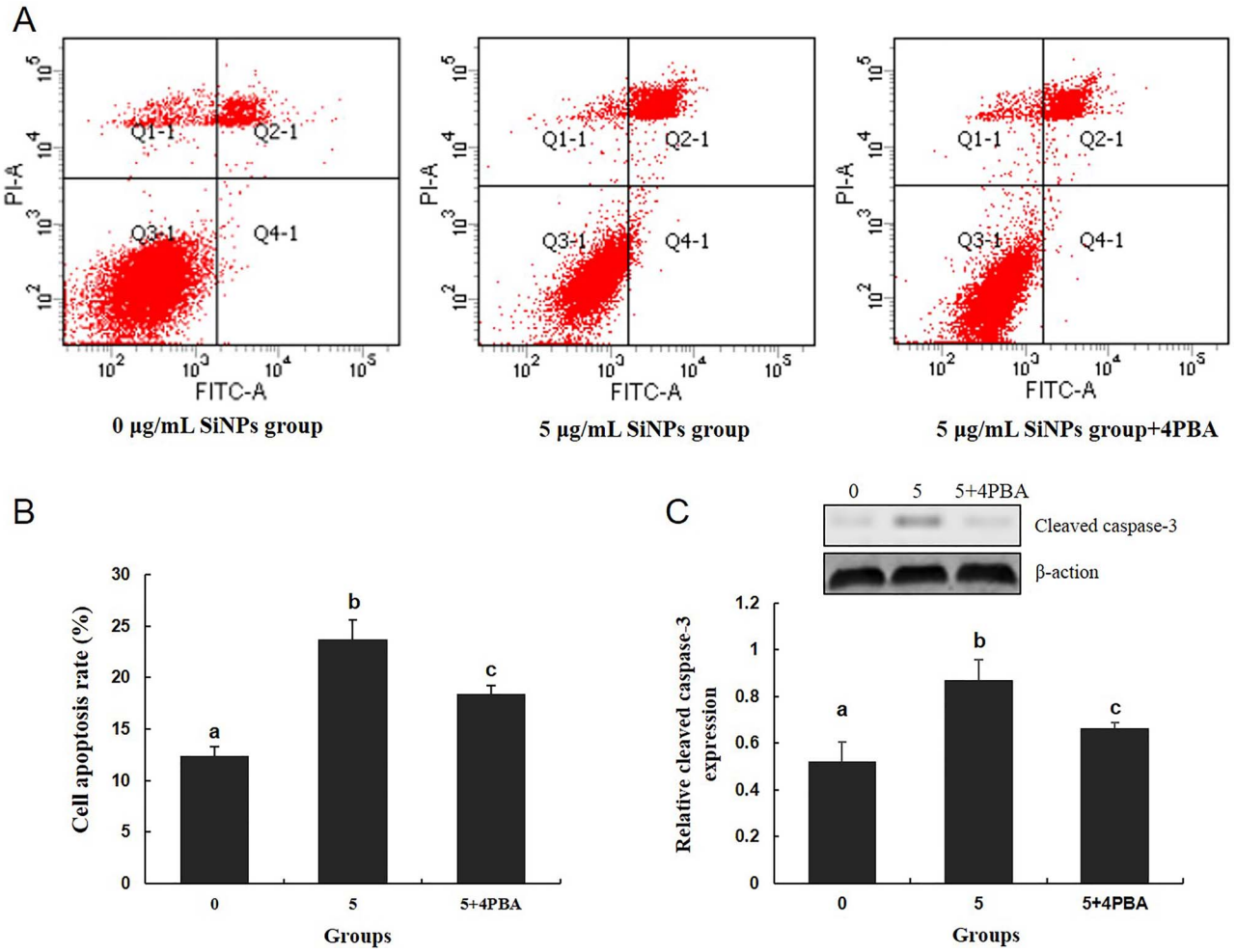


**Figure 5**: The effect of unfolded protein reaction inhibitor 4PBA on apoptosis and Cleaved caspase-3 in spermatocyte cells after exposure to SiNPs for 30 generations. Notes: **A**: The cell apoptosis was detected by a flow cytometry. **B**: The level of cell apoptosis. **C**: The protein expression of Cleaved caspase-3. 4PBA could inhibit SiNPs-induced cells apoptosis. The values with complete different superscript letters were significantly different among groups.

## Conclusion

In this study, cells were continuously exposed to SiNPs for 1, 10, 20 and 30 generations at the dose of 5 μg/ml SiNPs for 24 h per generation after attachment. With the increasing generation of exposure, SiNPs decreased the ability, induced the apoptosis of spermatocyte cells and increased the level of ROS; moreover, SiNPs increased the proteins expression of GRP-78, p-PERK, IRE1$\alpha$, ATF6 and Cleaved caspase-3 in spermatocyte cells, suggesting that SiNPs improved the UPR and apoptosis. The current results indicate that the long-term exposure to low-dose SiNPs could induce apoptosis by triggering ROS-mediated UPR in spermatocyte cells.

## Acknowledgements

This study was supported by the Beijing Natural Science Foundation Program and the Scientific Research Key Program of Beijing Municipal Commission of Education (KZ201510025028).

## Conflicts of interest

There are no conflicts of interest to declare.

## References

1. Sengupta P, Dutta S, Krajewska-Kulak E. The disappearing sperms: analysis of reports published between 1980 and 2015. *Am J Mens Health* 2017;**11**:1279–304.
2. Lafuente R, Garcia-Blaquez N, Jacquemin B *et al*. Outdoor air pollution and sperm quality. *Fertil Steril* 2016;**106**:880–96.
3. Cannarella R, Liuzzo C, Mongioi LM *et al*. Decreased total sperm counts in habitants of highly polluted areas of Eastern Sicily, Italy. *Environ Sci Pollut Res Int* 2019;**26**:31368–73.
4. Xue T, Zhu T. Association between fertility rate reduction and pre-gestational exposure to ambient fine particles in the United States, 2003–2011. *Environ Int* 2018;**121**:955–62.
5. Carre J, Gatimel N, Moreau J *et al*. Does air pollution play a role in infertility?: a systematic review. *Environ Health* 2017; **16**:82.
6. Duan J, Yu Y, Li Y *et al*. Inflammatory response and blood hypercoagulable state induced by low level co-exposure with silica nanoparticles and benzo[a]pyrene in zebrafish (*Danio rerio*) embryos. *Chemosphere* 2016;**151**:152–62.
7. Bitar A, Ahmad NM, Fessi H *et al*. Silica-based nanoparticles for biomedical applications. *Drug Discov Today* 2012;**17**:1147–54.

8. Schneider A, Hampel R, Ibald-Mulli A *et al*. Wichmann and A. Peters, changes in deceleration capacity of heart rate and heart rate variability induced by ambient air pollution in individuals with coronary artery disease. *Part Fibre Toxicol* 2010;**7**:29.
9. Mills NL, Tornqvist H, Gonzalez MC *et al*. Newby, ischemic and thrombotic effects of dilute diesel-exhaust inhalation in men with coronary heart disease. *N Engl J Med* 2007;**357**:1075–82.
10. Morishita Y, Yoshioka Y, Satoh H *et al*. Distribution and histologic effects of intravenously administered amorphous nanosilica particles in the testes of mice. *Biochem Biophys Res Commun* 2012;**420**:297–301.
11. Baki ME, Miresmaili SM, Pourentezari M *et al*. Effects of silver nano-particles on sperm parameters, number of Leydig cells and sex hormones in rats. *Iran J Reprod Med* 2014;**12**:139–44.
12. Ozgur ME, Ulu A, Ozcan I *et al*. Investigation of toxic effects of amorphous SiO2 nanoparticles on motility and oxidative stress markers in rainbow trout sperm cells. *Environ Sci Pollut Res Int* 2019;**26**:15641–52.
13. Leclerc L, Klein JP, Forest V *et al*. Blanchin and M, Cottier, testicular biodistribution of silica-gold nanoparticles after intramuscular injection in mice. *Biomed Microdevices* 2015;**17**:66.
14. Ren L, Zhang J, Zou Y *et al*. Silica nanoparticles induce reversible damage of spermatogenic cells via RIPK1 signal pathways in C57 mice. *Int J Nanomedicine* 2016;**11**:2251–64.
15. Zhang L, Wei J, Duan J *et al*. Silica nanoparticles exacerbates reproductive toxicity development in high-fat diet-treated Wistar rats. *J Hazard Mater* 2020;**384**:121361.
16. Roy A, Kumar A. ER stress and unfolded protein response in cancer cachexia. *Cancers (Basel)* 2019;**11**:1929.
17. Christen V, Fent K. Silica nanoparticles and silver-doped silica nanoparticles induce endoplasmatic reticulum stress response and alter cytochrome P4501A activity. *Chemosphere* 2012;**87**:423–34.
18. Wang J, Li Y, Duan J *et al*. Silica nanoparticles induce autophagosome accumulation via activation of the EIF2AK3 and ATF6 UPR pathways in hepatocytes. *Autophagy* 2018;**14**:1185–200.
19. Lee K, Lee J, Kwak M *et al*. Two distinct cellular pathways leading to endothelial cell cytotoxicity by silica nanoparticle size. *J Nanobiotechnol* 2019;**17**:24.
20. Ren L, Zhang J, Wang J *et al*. Silica nanoparticles induce spermatocyte cell apoptosis through microRNA-2861 targeting death receptor pathway. *Chemosphere* 2019;**228**:709–20.
21. Eom HJ, Choi J. Clathrin-mediated endocytosis is involved in uptake and toxicity of silica nanoparticles in Caenorhabditis elegans. *Chem Biol Interact* 2019;**311**:108774.
22. Edwards TM, Myers JP. Environmental exposures and gene regulation in disease etiology. *Environ Health Perspect* 2007;**115**:1264–70.
23. Bhatt RV. Environmental influence on reproductive health. *Int J Gynaecol Obstet* 2000;**70**:69–75.
24. Ren L, Liu J, Zhang J *et al*. Silica nanoparticles induce spermatocyte cell autophagy through microRNA-494 targeting AKT in GC-2spd cells. *Environ Pollut* 2019;**255**:113172.
25. Kim P, Scott MR, Meador-Woodruff JH. Dysregulation of the unfolded protein response (UPR) in the dorsolateral prefrontal cortex in elderly patients with schizophrenia. *Mol Psychiatry* 2019. https://doi-org-s.webvpn.bjmu.edu.cn/10.1038/s41380-019-0537-7.
26. Malhotra JD, Kaufman RJ. The endoplasmic reticulum and the unfolded protein response. *Semin Cell Dev Biol* 2007;**18**:716–31.
27. Schonthal AH. Targeting endoplasmic reticulum stress for cancer therapy. *Front Biosci (Schol Ed)* 2012;**4**:412–31.
28. Manie SN, Lebeau J, Chevet E. Cellular mechanisms of endoplasmic reticulum stress signaling in health and disease. 3. Orchestrating the unfolded protein response in oncogenesis: an update. *Am J Physiol Cell Physiol* 2014;**307**:C901–7.
29. Healy SJ, Gorman AM, Mousavi-Shafaei P *et al*. Targeting the endoplasmic reticulum-stress response as an anticancer strategy. *Eur J Pharmacol* 2009;**625**:234–46.
30. Lee KI, Lin JW, Su CC *et al*. Silica nanoparticles induce caspase-dependent apoptosis through reactive oxygen species-activated endoplasmic reticulum stress pathway in neuronal cells. *Toxicol In Vitro* 2019;**63**:104739.
31. N VR, Han HS, Lee H *et al*. ROS-responsive mesoporous silica nanoparticles for MR imaging-guided photodynamically maneuvered chemotherapy. *Nanoscale* 2018;**10**:9616–27.
32. Lin H, Liu XB, Yu JJ *et al*. Antioxidant N-acetylcysteine attenuates hepatocarcinogenesis by inhibiting ROS/ER stress in TLR2 deficient mouse. *PLoS One* 2013;**8**:e74130.
33. Wang Z, Wang H, Xu ZM *et al*. Cadmium-induced teratogenicity: association with ROS-mediated endoplasmic reticulum stress in placenta. *Toxicol Appl Pharmacol* 2012;**259**:236–47.
34. Lu TH, Su CC, Tang FC *et al*. Chloroacetic acid triggers apoptosis in neuronal cells via a reactive oxygen species-induced endoplasmic reticulum stress signaling pathway. *Chem Biol Interact* 2015;**225**:1–12.
35. Tang YH, Yue ZS, Zheng WJ *et al*. 4-Phenylbutyric acid presents therapeutic effect on osteoarthritis via inhibiting cell apoptosis and inflammatory response induced by endoplasmic reticulum stress. *Biotechnol Appl Biochem* 2018;**65**:540–6.
36. Mimori S, Okuma Y, Kaneko M *et al*. Protective effects of 4-phenylbutyrate derivatives on the neuronal cell death and endoplasmic reticulum stress. *Biol Pharm Bull* 2012;**35**:84–90.
37. Bohnert KR, Gallot YS, Sato S *et al*. Kumar, inhibition of ER stress and unfolding protein response pathways causes skeletal muscle wasting during cancer cachexia. *FASEB J* 2016;**30**:3053–68.
38. Gundamaraju R, Vemuri R, Chong WC *et al*. Interplay between endoplasmic reticular stress and survivin in colonic epithelial cells. *Cells* 2018;**10**:171.
39. Mimori S, Okuma Y, Kaneko M *et al*. Protective effects of 4-phenylbutyrate derivatives on the neuronal cell death and endoplasmic reticulum stress. *Biol Pharm Bul* 2012;**1**:84–90.
40. Li Y, Jiang W, Niu Q *et al*. eIF2$\alpha$-CHOP-BCl-2/JNK and IRE1$\alpha$-XBP1/JNK signaling promote apoptosis and inflammation and support the proliferation of Newcastle disease virus. *Cell Death Dis* 2019;**12**:891.
41. Liu X, Wu F, Du T *et al*. 4-phenylbutyric acid attenuates endoplasmic reticulum stress-mediated apoptosis and protects the hepatocytes from intermittent hypoxia-induced injury. *Sleep Breath* 2019;**2**:711–7.
42. Shigemi Z, Manabe K, Hara N *et al*. Watanabe and M. Fujimuro, Methylseleninic acid and sodium selenite induce severe ER stress and subsequent apoptosis through UPR activation in PEL cells. *Chem Biol Interact* 2017;**266**:28–37.
43. Bromati CR, Lellis-Santos C, Yamanaka TS *et al*. UPR induces transient burst of apoptosis in islets of early lactating rats through reduced AKT phosphorylation via ATF4/CHOP stimulation of TRB3 expression. *Am J Physiol Regul Integr Comp Physiol* 2011;**300**:R92–100.